View metadata, citation and similar papers at core.ac.uk
brought to you by CORE
provided by Bulletin of Electrical Engineering and Informatics

Bulletin of Electrical Engineering and Informatics
ISSN: 2302-9285
Vol. 5, No. 2, June 2016, pp. 194~204, DOI: 10.11591/eei.v5i2.529

Unrestricted Charging Controllar Design Magnitude

Amit Sachan*[1], Ashish Ranjan[2]
[1]Department of Electrical Engineering, China University of Mining & Technology, Xuzhou, China
[2]Department of Electrical Engineering, Arya Engineering College, India
*Corresponding author, e-mail: amitsachan55@gmail.com

Abstract

This paper presents to be routine in DC/DC phase of Bi-directional battery charger. The neutral is to analyst the filter latitude that will additional shrink the system cost and capacity. Key area is to moderate current ripple of the charging current which produce will approximately ripple unrestricted charging for batteries. Ripple unrestricted charging will shrink the further warmth triggered by the current ripple and surge the battery life. The filter-centered controller is project to transaction with the latent variability problem carried by a high order filter. The filter-centered technique has the compensations of effortlessly operation and no essential of additional current or voltage sensors. This dc/dc phase communicate converter to ease the charging purpose. Together low pass filter centered controller and nick filter based controller are evaluated and nick filter based controller has improved routine.

Keywords: *LCL filter, Bi-directional DC/DC phase Ripple factor, Unrestricted charging*

1. Introduction

A bi-directional battery charger can stand any a two-stage key or a single-stage resolution. Two-stage shows a bi-directional AC/DC phase then a bi-directional DC/DC phase. Aimed at a bi-directional AC/DC converter in equal 1 and level 2 power rating and voltage level, an H-bridge focused topology is archetypally expected. In this stage, collected non-isolated and isolated topology can be rummage sale. Half-bridge, full-bridge and push-pull are three edifice slabs, which are rummage sale to construct the non-isolated topologies [1]. Half-bridge centered buck boost topology is exploited [2]. Multi-phase half bridge based battery charger is projected for higher power rating charging claims [3, 4]. The idea can too decrease the passive components. DCM modulation has been rummage sale to decrease the size of the magnetic components to surge power density [5]. By complex DC bus voltage, multilevel DC/DC converter is planned to decrease the power losses and decrease the size of passive components [6]. Four-switch buck boost converter is planned to grip an extensive voltage range of battery [7]. Aimed at the non-isolated topology one point needs to be addressed. Due to safety obligation [4], all of the charging equipment must be isolated. Therefore, a charger with non-isolated DC/DC topology needs a line frequency transformer at the AC/DC phase. This low frequency transformer surges the bulk and volume of the charger. A high frequency transformer is rummage sale in isolated topologies to achieve galvanic isolation and soft switching as well.

The basic topologies include two bases at either primary side or secondary lateral: current source and voltage source [1]. Dual active bridge based topology is very prevalent [8]. Dual half bridge circuit is rummage-sale in lower power rating applications [9]. For high power applications, a three phase dual active bridge is planned [10, 11]. An inductor is used to form a current source in one side of the transformer and an active snubber is functional to decrease the voltage spike produced by this inductor [12, 13]. For isolated topologies, its compensations are higher power density and soft switching adept but the disadvantage is the loss of soft switching with different load situations. Contrary to a two-stage assembly, single stage topology will be a promising key which will decrease cost and surge system density. The controller design (as Figure 2) for single stage topology will be too a stimulating topic since the control structure is different compared to the well-defined two-stage converter control structure (as Figure 3).

Received November 27, 2015; Revised February 6, 2016; Accepted March 1, 2016

2. Dense Filter Latitude Ripple Unrestricted Charging

High demand filter cannot isolated be used in AC solicitation to shrink the filter size then can too be cast-off in battery charging solicitation. In kind of filter, two key parts are appreciated. Leading is the decrease of the filter size associated to conventional LC or L filter and vintage a compact battery charger. Second is the pledge the charging current has almost zero switching ripples. The ripple unrestricted charging can escape the negative assets carried by the high frequency current ripples. Yet adjacent is no substantial signal on the effect of ripple current on batteries, it is extensively hypothetical that ripple current may harm the asset of batteries subsequently him signs to temperature surges due to the auxiliary internal heating and power losses. Too, ripple currents may speed up positive grid corrosion and root premature anticlimaxes. Level ripple currents may have slight effect on conventional charging; their effect will be quite distinguished for the complex current charging or flat fast charging [14, 15, 16, 17]. Alternative vital concern is the cooling system expected at the battery bank. In self-propelled application, he is not practical to design an extra cooling system for battery bank. Thus it is not informal to yield obtainable the heat of the battery. Ripple unrestricted charging can shrink the heat of the battery, which assuages the load of the cooling system. In this paper ripple unrestricted current charging is attained by smearing an LCL filter [18, 19, 20] and this filter has an ample inferior value and size than conventional filter thru ripple currents. So a Dense magnitude and low volume charger can attain.

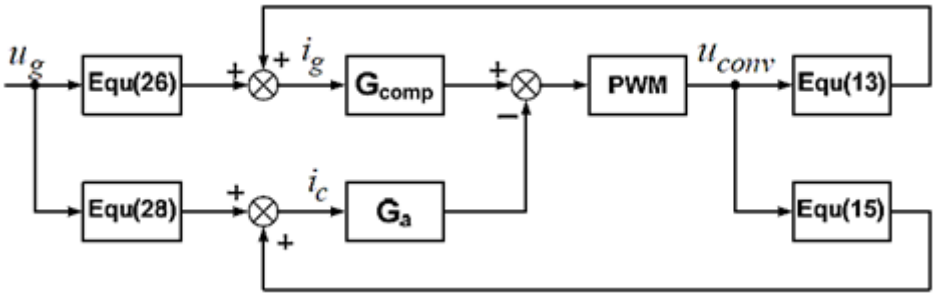

Figure 1. Block diagram of control plant and proposed controller

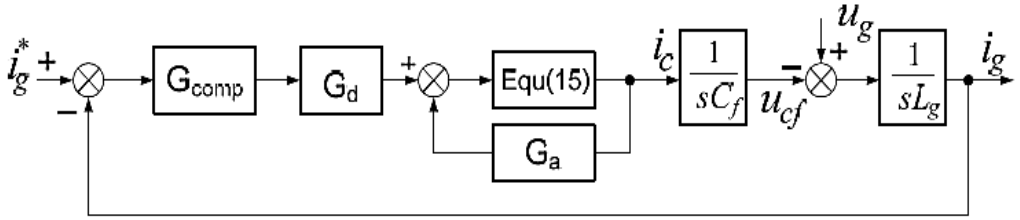

Figure 2. Control loop modeling

3. Filter Design

The spectrum of the PWM yield voltage of the dc/dc converter is written in (1)

$$u(t) = D.V_{dc} + \sum_{h=1}^{\infty} 2V_{dc} \frac{\sin(h\pi D)\cos(hwt)}{h\pi} \quad (1)$$

Set of battery with dc bus to design the converter side inductor, the charging current. The ripple current which is the half of the peak to peak current, so the converter side inductor can be chosen as a smaller value.

$$i_{L\_PK} = \frac{(V_{dc} - V_{batt})}{2L_1 f_s}.D \quad (2)$$

$$D = \frac{V_{batt}}{V_{dc}} \quad (3)$$

$$L_1 = \frac{(V_{dc} - V_{batt})}{2 f_s i_{L\_PK}}.D \quad (4)$$

The converter lateral current has ripple current and formerly the ripple current flows concluded a second order filter network calm by the capacitor C and battery side inductor L2. The ripple current will significantly reduce subsequently this LC network. To strategy this L2 and C, the transfer functions of converter cross current to converter output and battery side current to converter output are recycled. Deprived of as the confrontation of both inductors the transfer function is consequential:

$$\frac{i_1}{u_{conv}} = \frac{1 + L_2 C s^2}{L_1 L_2 C s^3 + (L_1 + L_2)s} \quad (5)$$

$$\frac{i_2}{u_{conv}} = \frac{1}{L_1 L_2 C s^3 + (L_1 + L_2)s} \quad (6)$$

Since these two transfer functions, the reduce ratio between the converter side current and the battery side current. In directive to achieve, ripple current lower.

$$\frac{i_2}{i_2} = \frac{1}{1 + L_2 C s^3} \quad (7)$$

$$L_1 = \frac{(V_{dc} - V_{batt})}{2 f_s i_{L\_PK}}.D \quad (8)$$

The conventional technique essential inductor produces to the equivalent current ripple. Then this inductor is 10 times the total inductance of L1 an L2. The inductor size for converter side inductor is essentially larger than theoretical size as of large current ripple on the inductor. The used Kool Mu core from Magnetics to design these inductors, First case the charging current equals, all the inductors are designed with E cores. Second case the charging current is amplified.

4. Controller Design

An unbroken current charging algorithm is design and implemented in digital controller. Its design and modeling technique is relatively analogous to the design of a grid-connected converter with LCL filter [18, 19]. To circumvent high frequency oscillation on the filter current, conventional controller needs to be altered. Then high frequency oscillation is bent by the converter PWM [20] output and the resonant frequency of LCL filter, a filter which is designed to extract and eradicate resonant frequency is plugged into the control loop. The virtues of this filter are that it functions deprived of additional current or voltage sensor, and it is laid-back to implement. For the filter form, any notch filter or low pass filter can used. The control loop prototypical is shown in Figure 3. The plant is deriving as below:

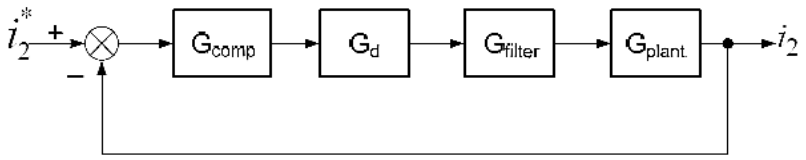

Figure 3. System Control loop model

$$\begin{cases} L_1 = \dfrac{di_1}{dt} = u_{conv} - u_c \\ L_2 = \dfrac{di_2}{dt} = u_c - u_{conv} \\ c.\dfrac{du_c}{dt} = i_1 - i_2 \end{cases} \quad (9)$$

In equation (9), L_1 is the converter side inductor, L_2 is the battery side inductor, and C is the filter capacitor. U_{conv} is the converter output voltage, U_c is the voltage on the filter capacitor, U_{batt} is the battery voltage. And i_1 is the converter side current and $i_2$is the battery side current and also the charging current. Transfer the equation (9) from time domain to frequency domain to get equation (10):

$$\begin{cases} L_1.i_1 s = u_{conv} - u_c \\ L_2.i_2 s = u_c - u_{conv} \\ c.u_c s = i_1 - i_2 \end{cases} \quad (10)$$

To get the small signal model, the battery voltage is assumed constant. Equation (9) can further derived to:

$$\begin{cases} u_{conv} = L_1.i_1 s + u_c \\ u_c = L_2.i_2 s \\ i_2 = i_1 + c.u_c s \end{cases} \quad (11)$$

From equation (11) substitute i_1 and U_c with i_2 and then derive the transfer function of charging current to converter output:

$$G_{plant}(s) = \frac{i_2}{u_{conv}} = \frac{1}{L_1 L_2 C s^3 + (l_1 + L_2)s} \quad (12)$$

The compensator used here is PI controller in equation (13):

$$G_{PI}(s) = K_P \frac{k_i}{s} \quad (13)$$

The propagation delay is model in equation (14)

$$G_d(s) = \frac{1}{1 + T.s} \quad (14)$$

In equation (14), the delay T is the switching cycle.

So the open loop transfer function of the system is written in equation (15) and bode plot is drawn in figure 2.

$$G(s) = G_{pi}(s)G_d(s)G_{plant}(s) \tag{15}$$

As we can see in figure 3 that Bode plot of the system with only PI compensation has a negative gain margin and is not stable. The high frequency gain in the system will yield high frequency resonant current on the charging current. In order to solve this issue, filter based method is proposed. The method can extract the resonant frequency and eliminate this frequency. Two types of filters are proposed. The first filter is a second order notch filter and its ideal transfer function is:

$$G_{filter} = \frac{s^2 + \omega^2{}_{res}}{s^2 + \frac{\omega_{res}.s}{Q_1} + \omega^2{}_{res}} \tag{16}$$

In the real system, this ideal transfer function will generate a very high negative magnitude at the setting frequency. So the transfer function is modifying to:

$$G_{filter\_notch} = \frac{s^2 + \frac{\omega_{res}.s}{d} + \omega_{res}^2}{s^2 + \frac{c.\omega_{res}.s}{d} + \omega_{res}^2} \tag{17}$$

The second filter used is a second order low pass filter and its transfer function is:

$$G_{filter\_low} = \frac{\omega_{res}^2}{s^2 + \frac{c.\omega_{res}.s}{Q_2} + \omega_{res}^2} \tag{18}$$

After plugging the notch filter transfer into the control loop the whole system transfer function:

$$G(s) = G_{pi}(s).G_d(s).G_{plant}(s).G_{filter\_notch}(s) \tag{19}$$

The notch filter resonant frequency matches the plant's resonant frequency precisely. We can get that subsequently smearing notch filter in the control loop; the phase boundary is close to the ideal phase edge for control system. The loop bandwidth is petite less than the switching frequency. The dc gain of the system is almost infinity because of a pole placed at zero frequency, which forms a first command system. By this controller the system will have high dc regulation accuracy and less steady-state error. The controller will have good dynamic response and a dumpy settling time as it is directly connected to a high phase boundary. The root locus of the system too verifies that the double-pole, which roots the system instability, is compensated with two zeros.

The low pass filter is the second proposed method. It purposes at plummeting all the magnitude subsequently its corner frequency. With its corner frequency tuned at the accurate value the high frequency peak is largely abridged. The control system with low pass filter is equation (20).

$$G(s) = G_{pi}(s).G_d(s).G_{plant}(s).G_{filter\_low}(s) \tag{20}$$

The Bode plot of the system, we can get that the low pass filter centered mode has the serious negative of low control bandwidth. The control bandwidth is slower than the notch filter

based method. In adding by the low pass filter the equal shifts to all frequencies subsequently solitary after its corner frequency but does not compensate for the resonant frequency peak. Therefore, here is option of improvement peaking at the resonant frequency. When amplified by improper improvement or system parameters the resonant increase will move higher than zero dB line which will lead to negative advantage margin and an unstable system the root locus plot too verifies that the resonant frequency is not compensated aimed at as the double-pole is very close to the borderline of the unit circle and oscillation is effortlessly generated. Centered on the study overhead the notch filter based method can attain improved recital than the low filter based method. The notch filter based method is too additional robust than the low pass filter based method. The robustness study and dynamic response for notch filter based controller will be observed.

5. Controller Robust Analysis

The controller by the notch filter is verifying to have improved routine than the low pass filter. Then frequently the notch filter is limited subsequently it can solitary be intended to be actual at a tapered frequency band. So if a system parameter such as inductance or capacitance has a sudden change, the controller routine of this technique is uncertain. In what way to spread frequency range and whether the extended frequency range disturbs controller routine will too be deliberated. The variation of inductance should emulate the variation of battery internal impedance.

The control loop by the notch filter conventional at the innovative value is associated with both capacitors. Once capacitance becomes larger the resonant frequency transfers to a lower frequency. We can perceive that prior to the notch filter resonant frequency here is a resonant peak and that peak will move across the zero dB line since the notch filter improvement at that frequency is not adequate to compensate for that frequency. Previously this resonant frequency the phase has previously passed -180 degree steadily as of the slow phase drop of the notch filter. So at this resonant frequency, level however the resonant peak crosses ended the zero dB line, the phase has previously dropped pointedly lower than -180. With numerous zero dB crossings, the first crossing is use to measure the bandwidth and phase margin. With the reduction of the capacitance, the resonant frequency is move to a higher frequency range. As we can see from the Bode plots, after the compensation from the notch filter the phase has a sudden jump above -180 degree because of the effect of resonant frequency. At -180 degree, crossing point the magnitude of the system is higher than dB so the negative gain margin leads to an unstable system. The notch filter has two parameters *c* and *d* in equation (17). They can use to control the magnitude and frequency range of the notch filter. By tuning *c* and *d* the frequency damping range is widened, A notch filter with different *c* and *d* parameters. System capacitance is stable because with a wider frequency damping range the magnitude is damped to be lower than dB even if the phase jumps back to -180 degree line. The bandwidth and phase of the system is determined by the first zero crossing point. The system with capacitance is still not stable because the frequency has moved to a higher level where the notch filter is ineffective for damping its magnitude. The gain margin becomes negative again and system is not stable. One way to make it stable is to retune the parameters to make the frequency damping range wider. The wider the damping range the lower the boosting phase. The phase will reduced with a wider damping range and we can see that although the system is stable the phase margin has already dropped to 36 degree that may lead to longer settling time and higher overshoot to the control loop.

The controller works well with low resonant frequency but has some drawbacks when the resonant frequency shifts to a higher frequency. By tuning the notch filter's parameters, the performance at the high frequency can be improve. This procedure phase margin is sacrifice. Tuning the notch filter can make the effective damping range wider but concurrently, the control system loses phase margin because of the notch filter. The effective frequency range of the notch filter, the system with capacitor can make stable. The notch filter is tune to widen the damped frequency range around the resonant frequency. So here is a tradeoff between the extension of the effective damped frequency range and control loop performance. To make the control loop robust to a wide range of parameters variation the control loop has too suffer from the phase margin reduction. The notch filter transfer function and the transfer function of control plant with all of the inductance. From the control loop design point of view, the variation of

capacitance is the same as the variation of inductance because both cases result in the movement of the resonant frequency. The inductance variation mainly comes from the inductor change because the internal inductance of the battery cannot chang drastically. We can see that the frequency variation resulting from the capacitance variation is wider than that of the inductance variation. So the capacitance variation can represent both the inductance and capacitance variation. The inductance variation analysis is the same as the capacitance variation so it is notincluded. The simulation is conduct to prove the above analysis. The Bode plot in that the controller for both capacitance has the same DC gain, phase margin and bandwidth. The capacitance changes from capacitance the charging current is well regulated but some low current ripples can observed. With the resonant frequency, moving toward an even lower frequency oscillation may be aroused. The redesigned notch filter the control system is stable. The charging current is regulated at the current ripples are higher because the filter capacitance becomes smaller and absorbs less ripple currents. The capacitance change from capacitance control system is no longer stable and the charging current begins to oscillate.

6. Simulation and Experiment

The simulation is conduct in Matlab Simulink with a 24V lead-acid battery pack. The circuit parameters are converter side inductor 0.1mH, the battery side inductor 0.0125mH, and the filter capacitor 40uF. The charging current is 5A, dc bus voltage is 50V, and the switching frequency is 5 kHz. As we can see the high frequency, oscillation appears on all currents. The blue curve is the converter side current, the purple curve is the capacitor current, and the red curve is the charging current. In Figure 4 the proposed controller is plug into the control loop, all currents are stable.

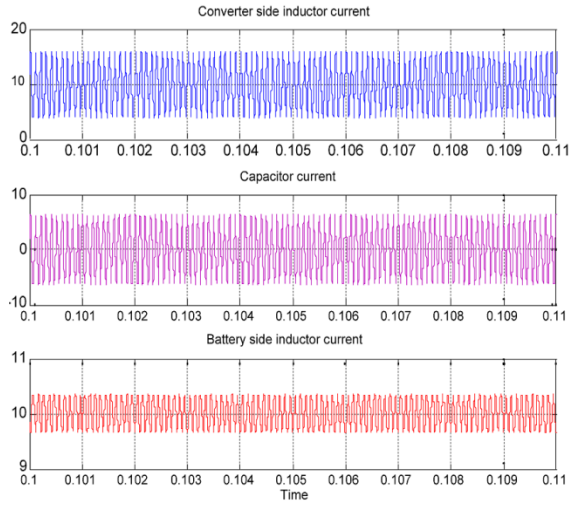

Figure 4. Simulation waveforms of three currentswithProposed control

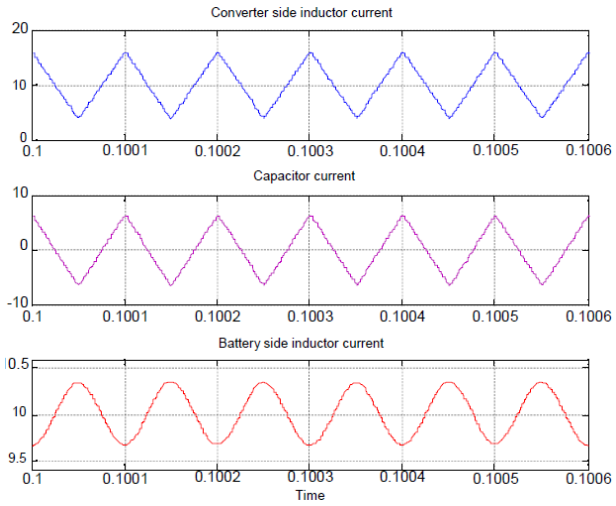

Figure 5. Zoom-in waveforms of three currents with proposed control

The zoom-in waveforms of three currents is shown in Figure 5. Experimental result for proposed control loop is shown in Figure 6 and the measured ripple current shown in Figure 7. Zoom-in waveforms of all three currents shown in Figure 8. So from the experiment results, we can see that converter side current has the peak-to-peak current ripple 6A, the capacitor current is 3A and the charging current has peak-to-peak current ripple 0.3 less than 1% of the charging current. Therefore, the target of ripple unrestricted charging is achiev. In Figure 9 the control loop dynamic response is tested.

In Figure 9 the charging current is changed from a low charging rate 1A (0.1C) to a high charging rate 10A (1C). The control objective is a battery bank, which has a quite slow response, but the control response speed is quite good. The settling time is less than 1ms and the current overshoot is less than 10%. The charging current is chang from a high charging rate 10A to a low charging rate 2A. In figure 10, the pulse-charging algorithm is implementing in the control loop. Since the tested battery is a lead-acid battery bank, the pulse frequency only needs several hundred hertz. Therefore, 100Hz current pulse charge is tested.

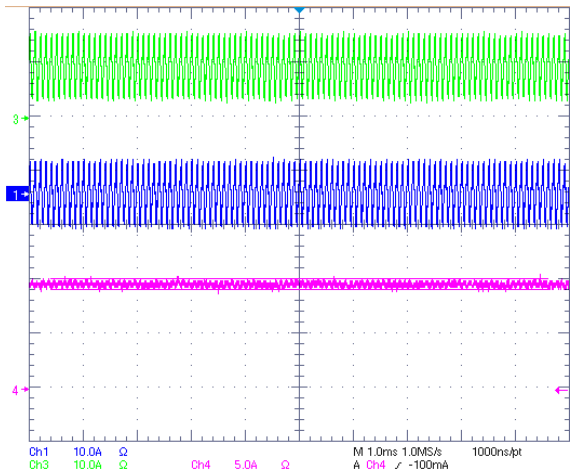

Figure 6. Experiment results of converter side current, charging Current and capacitor current with proposed control

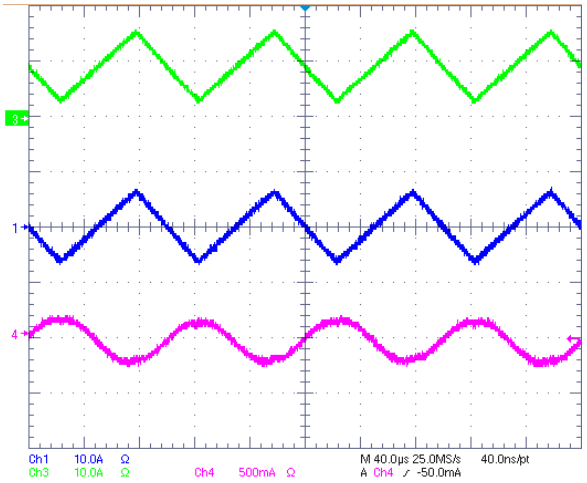

Figure 7. Experiment results of converter side current, charging current and capacitor current with proposed Control (charging current AC coupled to show ripple)

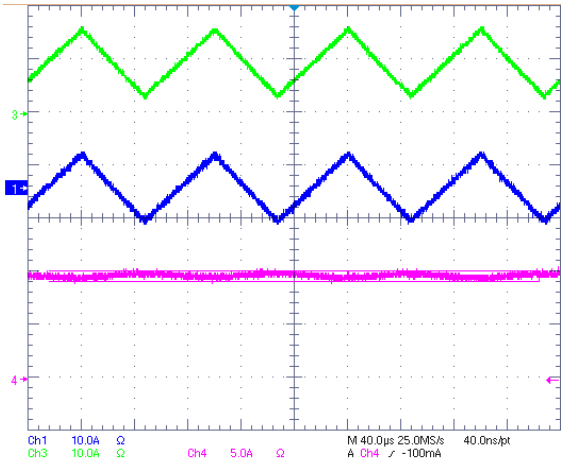

Figure 8. Experiment results of converter side current, charging current and capacitor current with proposed control (zoom-in)

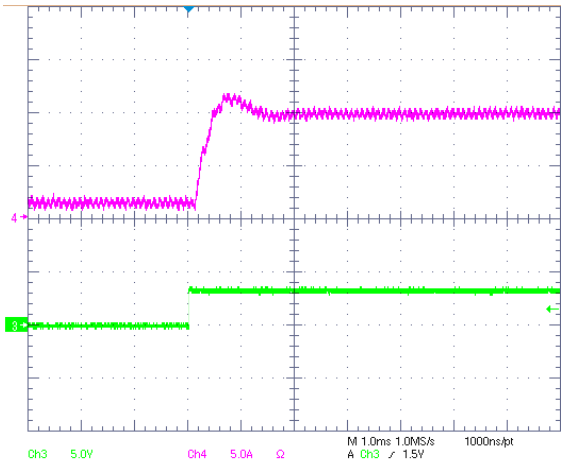

Figure 9. Experiment results of current transient response: 1A (0.1C) to 10A (1C) step change

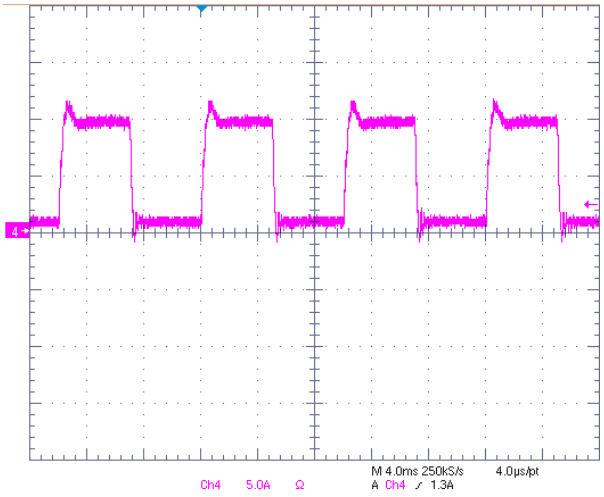

Figure 10. Experiment results of pulse charging with 100Hz

7. Conclusion

The key attainment of this high-order filter is to condense the filter scope and system volume and furthermore suggestively reduce the current ripples of the charging current which yield ripple unrestricted charging. Ripple unrestricted charging can decrease the heat generated thru the ripple current and internal resistance of the battery so it can lengthen the battery's generation. The resonance matter of the high demand filter, both the notch filter and low-pass filter centered controllers are projected and associated. Inclusive robustness analysis is conduct on the notch filter based controller. Simulation and experiment results verify the routine of the projected filter and innovative controller.

References

[1] Jih-Sheng Lai, DJ Nelson. "*Energy management power converters in hybrid electric and fuel cell vehicles*". IEEE Proceedings. 2007; 95(4): 766-777.
[2] Young-Joo Lee, A Khaligh, Ali Emadi. "Advanced integrated bidirectional AC/DC and DC/DC converter for plug-in hybrid electric vehicles". *IEEE Trans. Veh. Technol.* 2009; 58(8): 3970-3980.
[3] D Aggeler, F Canales, H Zelaya-De La Parra, A Coccia, N Butcher, O Apeldoorn. "*Ultra-fast DCcharge infrastructure for EV-mobility and future smart grids*". in Proc IEEE ISGT Europe. 2010: 1-8.
[4] DP Urciuoli, CW Tipton. "*Development of a 90 kW Bi-directional DC-DC Converter for Power Dense Applications*". in Proc IEEE APEC'06. 2006: 1375-1378.
[5] M Pepper, K Mansfield, J Elmes, K Rustom, etc. "*Bi-directional DCM DC to DC Converter for Hybrid Electric Vehicles*". in Proc IEEE PESC'08. 2008: 3088-3092.
[6] S Waffler, JW Kolar. "A Novel Low-Loss Modulation Strategy for High-Power Bidirectional Buck Boost Converter". IEEE Trans. Power Electron. 2009; 24(6): 1589-1599.
[7] Mustansir H Kheraluwala. "High-Power High-Frequency DC-To-DC Converters". Dissertation, University of Wisconsin-Madison. 1991.
[8] Fang Z Peng, Hui Li, Gui-Jia Su an Jack S Lawler. "A new ZVS bidirectional DC-DC converter for fuel cell and battery application". *IEEE Trans. Power Electron*. 2004; 19(1): 54-65.
[9] MN Kheraluwala, RW Gascoigne, DM Divan, ED Baumann. "Performance characterization of a high-power dual active bridge dc-to-dc conveter". *IEEE Trans. Ind. Appl*. 1992; 28(6): 1294-1301.
[10] RW AA De Doncker, DM Divan, MH Kheraluwala. "A three-phase soft-switched high-powerdensity dc/dc converter for high-power applications". *IEEE Trans. Ind. Appl*. 1991; 27(1): 63-73.
[11] Lizhi Zhu. "A novel soft-commutating isolated boost full-bridge zvs-pwm dc-dc converter for bidirectional high power applications". *IEEE Trans. Power Electron*. 2006; 21(2): 422-429.
[12] Lizhi Zhu, Kunrong Wang, Fred C Lee, Jin-Sheng Lai. "New start-up schemes for isolated full-bridge boost converters". *IEEE Trans. Power Electron*. 2003; 18(4): 946-951.
[13] F Katiraei, MR Iravani. "Power management strategies for a microgrid with multiple distributed generation unites". *IEEE Trans. Power Syst*. 2006; 21(4): 1821-1831.
[14] AI Harrison. "Batteries and AC phenomena in UPS systems: the battery point of view". in *IEEE 1989 Telecommunications Energy Conference*. 1989.

[15] Effects of AC ripple current on VRLA battery life. Emerson Network Power.
[16] Nasser Kutkut. "Output AC ripple effects". Technical Note, Power Designers.
[17] KH Ahmed, AM Massoud, SJ Finney, BW Williams. "A Modified Stationary Reference Framebased Predictive Current Control with Zero Steady-State Error for LCL Coupled Inverter-based Distributed Generation Systems". *IEEE Trans. Ind. Electron.* 2011; 58(4): 1359-1370.
[18] C Wessels, J Dannehl, FW Fuchs. "Active Damping of LCL-Filter Resonance based on Virtual Resistor for PWM Rectifier-Stability Analysis with Different Filter Parameters". *in Proc IEEE PESC'08*. 2008: 3532-3358.
[19] W Gullvik, L Norum, R Nilsen. "Active Damping of Resonance Oscillation in LCL-Filters based on Virtual Flux and Virtual Resistor". *in Proc. IEEE EPE'07*. 2007.
[20] Qingrong Zeng, Liuchen Chang. "An Advanced SVPWM-based Predictive Current Controller for Three- Phase Inverters in Distributed Generation Systems". *IEEE Trans. Ind. Electron.* 2008; 55(3): 1235-1246.